position and anisotropy of the UHE CR flux to be measured, which would provide additional information on its origin.

REFERENCES AND NOTES

1. K. Greisen, *Phys. Rev. Lett.* **16**, 748 (1966); G. T. Zatsepin and V. A. Kuzmin, *Pis'ma Zh. Eksp. Teor. Fiz.* **4**, 114 (1966) [*J. Exp. Theor. Phys.* **4**, 78 (1966)]; F. W. Stecker, *Phys. Rev. Lett.* **21**, 1016 (1968).
2. J. L. Puget, F. W. Stecker, J. H. Bredekamp, *Astrophys. J.* **205**, 638 (1976).
3. M. Nagano and F. Takahara, Eds., *Astrophysical Aspects of the Most Energetic Cosmic Rays* (World Scientific, Singapore, 1991).
4. Proceedings of the *Tokyo Workshop on Techniques for the Study of Extremely High Energy Cosmic Rays*, Tokyo, 27 to 30 September 1993 (Institute for Cosmic Ray Research, Univ. of Tokyo, 1993).
5. M. A. Lawrence, R. J. O. Reid, A. A. Watson, *J. Phys. G Nucl. Part. Phys.* **17**, 733 (1991); A. A. Watson, in (*3*), p. 2.
6. N. N. Efimov *et al.*, in (*3*), p. 20; T. A. Egorov, in (*4*), p. 35.
7. D. J. Bird *et al.*, *Phys. Rev. Lett.* **71**, 3401 (1993); *Astrophys. J.* **424**, 491 (1994).
8. D. J. Bird *et al.*, *Astrophys. J.* **441**, 144 (1995).
9. S. Yoshida *et al.*, *Astropart. Phys.* **3**, 105 (1995).
10. N. Hayashida *et al.*, *Phys. Rev. Lett.* **73**, 3491 (1994).
11. J. P. Rachen, T. Stanev, P. L. Biermann, *Astron. Astrophys.* **273**, 377 (1993); J. W. Elbert and P. Sommers, *Astrophys. J.* **441**, 151 (1995).
12. G. Sigl, D. N. Schramm, P. Bhattacharjee, *Astropart. Phys.* **2**, 401 (1994).
13. F. Halzen, R. A. Vazquez, T. Stanev, H. P. Vankov, *ibid.* **3**, 151 (1995).
14. A. M. Hillas, *Annu. Rev. Astron. Astrophys.* **22**, 425 (1984).
15. C. A. Haswell, T. Tajima, J.-I. Sakai, *Astrophys. J.* **401**, 495 (1992).
16. S. Yoshida and M. Teshima, *Prog. Theor. Phys.* **89**, 833 (1993).
17. P. Bhattacharjee, C. T. Hill, D. N. Schramm, *Phys. Rev. Lett.* **69**, 567 (1992).
18. F. A. Aharonian, P. Bhattacharjee, D. N. Schramm, *Phys. Rev. D* **46**, 4188 (1992).
19. J. Geddes, T. C. Quinn, R. M. Wald, *Astrophys. J.*, in press.
20. D. J. Bird *et al.*, Proceedings of the *Twenty-Fourth International Cosmic Ray Conference*, Rome, 28 August to 8 September 1995 (Instituto Nazionale Fisca Nucleare, Rome, 1995), vol. 2, pp. 504–507.
21. Proceedings of the International Workshop on Techniques to Study Cosmic Rays with Energies $\geq 10^{19}$ eV, Paris, 22 to 24 April 1992, M. Boratav *et al.*, Eds., *Nucl. Phys. B* **28B** (1992), (Proc. suppl.).
22. G. Sigl and S. Lee, in (*20*), pp. 356–359.
23. S. Lee and G. Sigl, in preparation.
24. T. A. Clark, L. W. Brown, J. K. Alexander, *Nature* **228**, 847 (1970).
25. X. Chi, C. Dahanayake, J. Wdowczyk, A. W. Wolfendale, *Astropart. Phys.* **1**, 239 (1993); G. Sigl, K. Jedamzik, D. N. Schramm, V. S. Berezinsky, Fermilab publication 95/051-A, *Phys. Rev. D.*, in press; R. J. Protheroe and P. A. Johnson, *Astroparticle Phys.*, in press.
26. C. T. Hill and D. N. Schramm, *Phys. Rev. D* **31**, 564 (1985).
27. For a recent account see, for example, C. A. Norman, D. B. Melrose, A. Achterberg, *Astrophys. J.* **454**, 60 (1995).

28. We gratefully acknowledge J. W. Cronin, S. Yoshida, and P. Sommers for reading the manuscript and giving valuable suggestions. Supported by the Department of Energy (DOE), NSF, and the National Aeronautics and Space Administration (NASA) at the University of Chicago, by the DOE and by NASA through grant NAG5-2788 at Fermilab, and by the Alexander-von-Humboldt Foundation. S.L. acknowledges the support of the POSCO Scholarship Foundation in Korea. P.B. wishes to thank R. Kolb and J. Frieman for hospitality and support at Fermilab at the beginning stages of this work.

12 June 1995; accepted 14 September 1995

Selective Trafficking of KNOTTED1 Homeodomain Protein and Its mRNA Through Plasmodesmata

William J. Lucas,* Sabine Bouché-Pillon, David P. Jackson, Lynda Nguyen, Lucian Baker, Biao Ding,† Sarah Hake

Plasmodesmata are intercellular organelles in plants that establish cytoplasmic continuity between neighboring cells. Microinjection studies showed that plasmodesmata facilitate the cell-to-cell transport of a plant-encoded transcription factor, KNOTTED1 (KN1). KN1 can also mediate the selective plasmodesmal trafficking of *kn1* sense RNA. The emerging picture of plant development suggests that cell fate is determined at least in part by supracellular controls responding to cellular position as well as lineage. One of the mechanisms that enables the necessary intercellular communication appears to involve transfer of informational molecules (proteins and RNA) through plasmodesmata.

Cell fate in higher plants is determined by position rather than by lineage (*1*). Although environmental and hormonal signals could act in a cell-autonomous manner to control cell fate, clonal analysis of developmental mutants has indicated that cell-to-cell transport, as part of a longer chain of signaling events, may be involved in the orchestration of developmental events (*2*). For example, expression of the gene *Floricaula* (to produce FLO), which affects meristem identity in *Antirrhinum majus* (snapdragon) in only the outer (epidermal) layer (L1) of the meristem, activates downstream genes involved in flower development (*3*) in adjacent cell layers. Similarly, the genotype of the inner layer (L3) of the tomato floral meristem controls development of the outer layers (L2 and L1) (*4*). These findings are consistent with the hypothesis that FLO and the fasciated gene product of tomato potentiate cellular interactions among the three layers of the floral meristem.

Although such intercellular control may be mediated by cell surface receptors and soluble ligands, it may also involve the selective cell-to-cell transport of proteins through plasmodesmata, the specialized, plasma membrane–lined cytoplasmic pores that maintain cytoplasmic and endomembrane continuity between many cells in the plant (*5*). These pores are the route by which viral movement proteins, which are essential for the spread of infection in plants (*6*), mediate trafficking of viral RNA and DNA (*6*–*8*). The viral movement proteins seem to interact with an endogenous plasmodesmal macromolecular trafficking pathway.

Here we report an analysis of movement of the protein and RNA encoded by the maize *knotted1* (*kn1*) homeobox gene (*9*). Ectopic expression of *kn1* in the vascular tissue of

W. J. Lucas, S. Bouché-Pillon, L. Nguyen, L. Baker, B. Ding, Section of Plant Biology, Division of Biological Sciences, University of California, Davis, CA 95616, USA. D. P. Jackson and S. Hake, U.S. Department of Agriculture–University of California Berkeley Plant Gene Expression Center, Albany, CA 94710, USA.

*To whom correspondence should be addressed.
†Present address: Department of Botany, Oklahoma State University, Stillwater, OK 74078, USA.

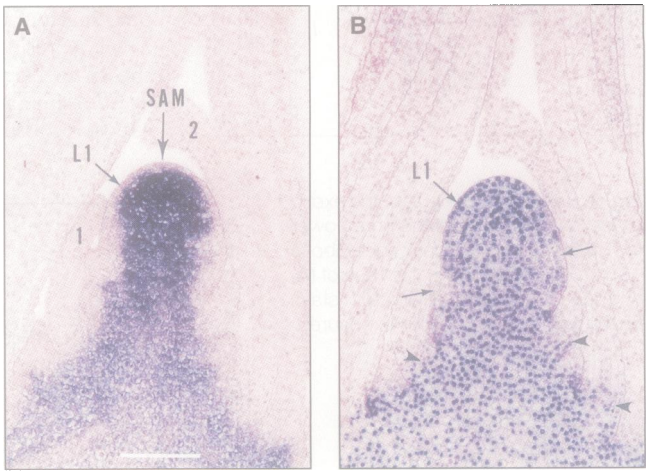

Fig. 1. Serial sections of a maize vegetative shoot apex processed for in situ hybridization for *kn1* mRNA (**A**) and immunolocalization of KN1 (**B**) reveal the presence of KN1 in L1 cells in which its mRNA is not detected. The shoot apical meristem (SAM) is flanked by leaf primordia [1 and 2 in (A)] and older expanding leaves in which *kn1* mRNA and KN1 are not detected. Regions in the SAM that lack KN1 [unlabeled arrows in (B)] predict the position of leaf primordial development. L1, outer cell layer of the SAM. Note that KN1 is present in a few cells across the base of each developing leaf (arrowheads). Scale bar, 100 μm.

developing maize leaves alters cell differentiation within adjacent mesophyll and epidermal layers, which suggests that a signal moves from one cell layer to another. In situ and immunolocalization studies of the maize shoot apical meristem (*10*) demonstrated that *kn1* mRNA was detected only within the interior (L2) cells of the meristem, whereas KN1 was detected in the L2 cells and in the epidermal (L1) layer [Fig. 1, A and B (*11*)]. These results suggested that, despite the fact that KN1 is a nuclear-localized transcription factor, the KN1 protein itself might be the signal that is transported from L2 into L1, as well as between cell layers in knotted leaves.

Escherichia coli–expressed KN1 labeled with fluorescein isothiocyanate (FITC-KN1) (*12*) was microinjected into the cytoplasm of plant cells (*13*). The small size of the cells in the maize shoot apical meristem precluded us from performing microinjection experiments on such tissues. Instead, we used developing maize leaves and microinjected mesophyll cells connected to the vascular bundle, as this was the site where ectopically expressed *kn1* had been shown to alter cell fate (9). FITC-KN1 injected into the cytoplasm of these mesophyll cells moved into bundle sheath cells and surrounding mesophyll cells (Table 1). Thus, KN1 must be capable of interacting with plasmodesmata to potentiate its own movement from cell to cell. Tobacco offers another system in which to study KN1, as ectopic meristems are also obtained when KN1 is overexpressed in tobacco (*14*). FITC-KN1 microinjected into mesophyll cells of tobacco (*Nicotiana tabacum* cv. Samsun) leaves also moved to neighboring cells (Fig. 2A and Table 2). Cell-to-cell movement of injected Lucifer yellow CH (molecular weight, 457), a membrane-impermeant fluorescent probe, established that plasmodesmata in the injected tissues displayed normal characteristics (*15*) (Tables 1 and 2). Furthermore, the lack of movement of FITC-labeled bacterial proteins established that KN1 movement was not an artifact of the preparative techniques used (Table 2).

An increase in the plasmodesmal size exclusion limit (SEL) is required for cell-to-cell transport of viral movement proteins (6–8). An increase in plasmodesmal SEL is also associated with KN1 cell-to-cell movement in maize and tobacco (Tables 1 and 2). Microinjection of 9.4 or 20 kD of FITC-labeled dextran alone did not result in movement out of the injected cell (Fig. 2C), but coinjection of these FITC-dextrans with unlabeled KN1 gave rise to the same spread of fluorescence as was detected when FITC-KN1 was introduced into the cell (Fig. 2, A and D, and Tables 1 and 2). This KN1-induced increase in plasmodesmal SEL also permitted the cell-to-cell movement of a labeled, coinjected, 20-kD

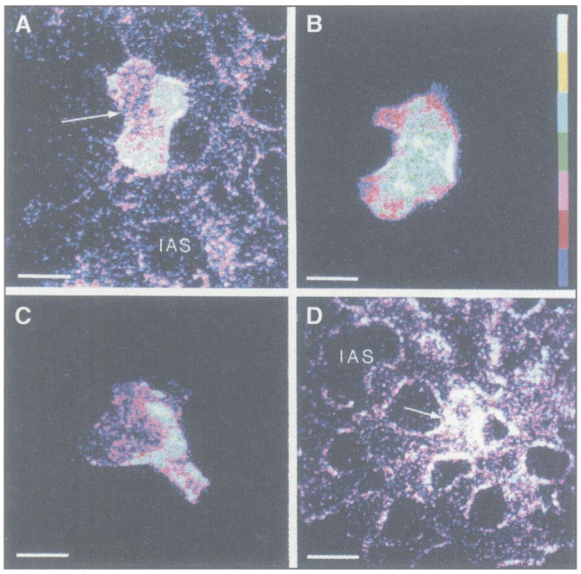

Fig. 2. Cell-to-cell transport of FITC-KN1 and its effect on plasmodesmal SEL in tobacco mesophyll cells. KN1 and its mutant derivative, M6 (see Fig. 3), were expressed in *E. coli* and extracted proteins were labeled with FITC before being used in microinjection studies. Immediately after being introduced into a tobacco mesophyll cell, FITC-labeled KN1 moved into surrounding cells as indicated by false-color imaging (**A**) obtained with a Hamamatsu model C1966 analytical system (*7, 8*). (**B**) Containment of FITC-labeled M6, 15 min after injection into the cell. (**C**) Injected 20-kD FITC-dextran remained indefinitely (60 min after injection) within the target cell. (**D**) Coinjection of 20-kD FITC-dextran and unlabeled KN1 resulted in extensive movement (image taken 2 min after injection). Arrows identify injected cells; IAS, intercellular air space. Color bar: background is black, and pale blue and yellow represent the higher intensity of fluorescence observed (the bar is common to Figs. 2 and 4). Scale bar in (A), 25 μm; (B), 20 μm; (C), 25 μm; and (D), 50 μm.

Table 1. KN1 interacts with plasmodesmata to increase the SEL of maize mesophyll cells and potentiates its own cell-to-cell transport. The normal SEL of plasmodesmata in such plant cells is 800 to 100 daltons (*5*). The largest material known to pass through mesophyll plasmodesmata is a viral movement protein of 35 kD (*6*). Developing maize leaves (1 to 2 cm in width) from young seedlings (14 days after germination) were used in these experiments.

Injected material	Microinjections	
	Total (*n*)	Movement* [*n* (%)]
Lucifer yellow CH	12	11 (92)
FITC-KN1	12	10 (83)
9.4-kD FITC-dextran	12	1 (8)
KN1 + 9.4-kD FITC-dextran	11	9 (82)

*Number of injections [see (*13*)] and percent of total injections in which the fluorescently labeled probe moved from the injected cell into surrounding tissue. Fluorescence was detected with a Leitz Orthoplan epi-illumination microscope coupled with a Hamamatsu model C1966-20 analytical system, and permanent images were recorded on videotape.

Table 2. KN1 interacts with plasmodesmata to increase the SEL of tobacco mesophyll cells and potentiates its own cell-to-cell transport.

Injected material	Microinjections	
	Total (*n*)	Movement* [*n* (%)]
Lucifer yellow CH	54	49 (91)
FITC-KN1	33	29 (88)
FITC-labeled bacterial proteins	10	0 (0)
9.4-kD FITC-dextran	35	3 (9)
KN1 + 9.4-kD FITC-dextran	38	29 (76)
20-kD FITC-dextran	11	1 (9)
KN1 + 20-kD FITC-dextran	19	16 (84)
KN1 + 39-kD FITC-dextran	25	5 (20)
20-kD FITC-soybean trypsin inhibitor	15	2 (13)
KN1 + 20-kD FITC-soybean trypsin inhibitor	10	10 (100)
FITC-KN1 (M6)†	15	1 (7)
KN1 (M6) + 9.4-kD FITC-dextran	16	3 (19)
KN1 (M1) + 9.4-kD FITC-dextran	11	8 (73)
KN1 (M2) + 9.4-kD FITC-dextran	8	6 (75)
KN1 (M3) + 9.4-kD FITC-dextran	8	6 (75)
KN1 (M4) + 9.4-kD FITC-dextran	12	8 (75)
KN1 (M5) + 9.4-kD FITC-dextran	9	9 (100)
KN1 (M7) + 9.4-kD FITC-dextran	7	6 (86)
KN1 (M8) + 9.4-kD FITC-dextran	8	6 (75)
KN1 (M9) + 9.4-kD FITC-dextran	16	10 (63)

*Number of injections [see (*13*)] and percent of total injections in which the fluorescently labeled probe moved from the injected cell into surrounding tissue. Movement of fluorescently labeled *kn1* mRNA or of CMV RNA was detected as described in Table 1. †Details on the amino acid changes engineered for each KN1 mutant are given in Fig. 3.

soybean cytosolic protein, soybean trypsin inhibitor (Table 2). Occasionally, KN1 permitted the movement of a 39-kD FITC-dextran, and so the upper plasmodesmal SEL associated with KN1 transport is greater than 20 kD and close to 39 kD.

Protein domains essential for KN1 cell-to-cell movement were investigated with the use of a series of alanine scanning mutants (*12*) (Fig. 3). Of the nine mutants studied, only one (M6) showed a substantial reduction in ability to move from cell to cell (Fig. 2B and Table 2). The M6 mutation resides in a potential nuclear localization sequence that is present in the NH_2-terminal region of the homeodomain (*16*). Determination of whether this reflects homology between nuclear and plasmodesmal transport systems must await the identification and characterization of other transcriptional regulators that also have the capacity for plasmodesmal transport.

Although the other mutants of KN1 retained the capacity to dilate plasmodesmata and potentiate their own cell-to-cell transport (Table 2), the rate and extent of movement of each mutant KN1 was reduced as compared with those of wild-type KN1. FITC-KN1 was routinely detected in neighboring cells 1 to 2 s after its injection into a mesophyll cell, with further movement through 5 to 10 surrounding cells seen in approximately 30 s. Although the period before each mutant FITC-KN1 could be detected in the neighboring cells was also short (a few seconds), subsequent movement into the second layer of cells required from 3 to 5 min. Furthermore, rarely did we detect fluorescence beyond this second layer of mesophyll cells. Analysis of plant viral movement proteins (6–8), on the other hand, showed that alanine scanning mutants either exhibited normal movement or were incapable (0% movement) of cell-to-cell transport. The varied response of KN1 mutants may reflect the presence of multiple domains involved in mediating efficient plasmodesmal transport or interaction with the plasmodesmata.

Having established that KN1 interacts with plasmodesmata to increase SEL and mediate in its own cell-to-cell transport, characteristics that are held in common with many viral movement proteins (6–8), we next investigated whether KN1 could also mediate trafficking of nucleic acids, although the results in Fig. 1 suggest no such ability. Sense *kn1* RNA was TOTO-labeled (RNA-TOTO) (*17*) and coinjected into mesophyll cells with unlabeled KN1. In the presence of KN1, the fluorescence associated with *kn1* sense RNA-TOTO moved as rapidly and extensively from cell to cell as did FITC-KN1 when it alone was injected into this tissue (Fig. 4). Control microinjection experiments involving *kn1* sense RNA-TOTO alone, *kn1* antisense RNA-TOTO alone, or unlabeled KN1 plus *kn1* antisense RNA-TOTO established the specificity of KN1-mediated *kn1* RNA transport, because in each of these cases the fluorescent probes remained in the injected cell (Fig. 4B and Table 3). The M6 mutant of KN1, which

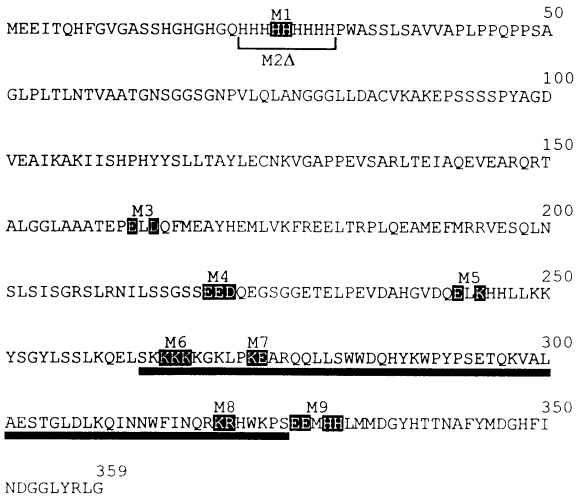

Fig. 3. KN1 alanine scanning and deletion mutants generated to identify the protein domain or domains essential for KN1-plasmodesmal interaction (*12*). Amino acid residues (*20*) changed to alanines are marked with black boxes, with the assigned number of each mutant indicated above the site. Deletion mutant M2 was generated by the removal of a nine-histidine stretch from positions 22 to 30. The residues associated with the KN1 homeodomain (*16*) are underlined. The domains affected by these mutations are as follows: M1 and M2, histidine-rich region of unknown function; M3 and M4, regions conserved between certain *kn1*-related genes; M5, the "ELK" region, which is conserved in all KN1-like homeodomain proteins (*16*); M6, potential nuclear localization sequence; M7, homeodomain first helix; M8, homeodomain third helix; and M9, COOH-terminal border of homeodomain (*16*).

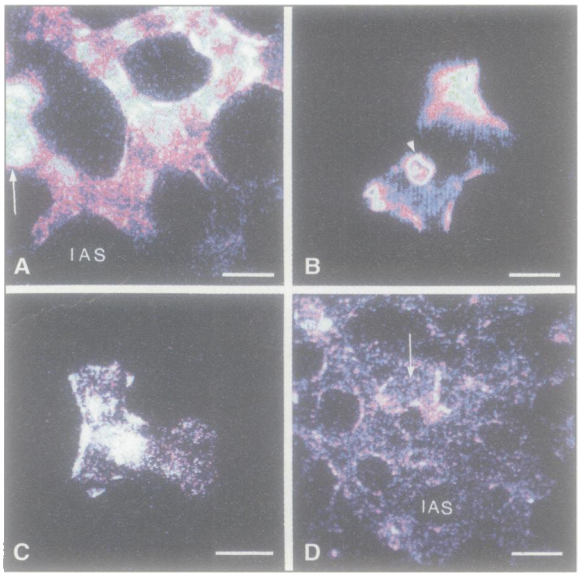

Fig. 4. KN1 protein-mediated cell-to-cell transport of *kn1* RNA-TOTO. (**A**) Coinjection of KN1 and *kn1* sense RNA-TOTO into a tobacco mesophyll cell revealed movement of the *kn1* sense RNA-TOTO into cells in the vicinity of the injected cell (arrow) after 1 min. IAS, intercellular air space. (**B**) *Kn1* antisense RNA-TOTO failed to move out of the target cell when coinjected with KN1. The false-color image was taken 15 min after coinjection, at which time fluorescence had accumulated in what appeared to be the nucleus (arrowhead). (**C**) Tobacco mesophyll cell coinjected with KN1 and CMV RNA-TOTO (*18*) after 15 min. Fluorescence remains confined to the injected cell. Although KN1 would presumably have trafficked into surrounding cells, it failed to transport the CMV RNA-TOTO. (**D**) Coinjection of CMV 3a movement protein and *kn1* sense RNA-TOTO into a tobacco mesophyll cell (arrow) resulted in extended CMV 3a movement protein–mediated transport of the *kn1* sense RNA-TOTO into the surrounding cells 2 min after injection. Scale bar in (A), 35 μm; (B), 20 μm; (C), 25 μm; and (D), 50 μm.

Table 3. KN1 can selectively traffic its own mRNA through plasmodesmata. MP, movement protein.

Injected material	Microinjections	
	Total (*n*)	Movement* [*n* (%)]
kn1 sense RNA-TOTO	25	1 (4)
kn1 sense RNA-TOTO plus KN1	22	20 (91)
kn1 sense RNA-TOTO plus KN1 M6	10	0 (0)
kn1 antisense RNA-TOTO	10	2 (20)
kn1 antisense RNA-TOTO plus KN1	10	0 (0)
CMV RNA-TOTO plus CMV 3a MP	15	13 (87)
CMV RNA-TOTO plus KN1	15	3 (20)
kn1 sense RNA-TOTO plus CMV 3a MP	15	12 (80)

*Number of injections and percent of total injections in which *kn1* mRNA or CMV RNA moved from target cell into surrounding tissue. Movement of fluorescently labeled *kn1* mRNA or of CMV RNA was detected as described in Table 1.

was least able to transport itself, did not potentiate the cell-to-cell transport of *kn1* sense RNA-TOTO (Table 3).

KN1 was selective in terms of the RNA that it would traffic, as shown by coinjection of TOTO-labeled cucumber mosaic virus (CMV) single-stranded sense RNA (*18*) and KN1 (Fig. 4C, Table 3). The CMV movement protein, in contrast, potentiated cell-to-cell transport both of its own RNA and of *kn1* RNA (Fig. 4D, Table 3), which is consistent with the known nonspecificity of viral movement proteins (*6*–*8*).

Our finding that KN1 has the capacity to move from cell to cell provides a possible explanation for the lack of cell autonomy seen with the dominant *Kn1* mutation as well as with other developmental mutations (*3*, *4*, *19*). How such plasmodesmal transport is controlled to create developmental domains (*5*) remains to be elucidated. The extent to which a transcription factor can move within a tissue may be controlled by the presence of proteins that regulate its plasmodesmal and nuclear pore transport. This might explain why, in the maize meristem, KN1 was present in both L1 and L2 nuclei (Fig. 1), whereas in tobacco mesophyll cells, microinjected FITC-KN1 moved preferentially through plasmodesmata rather than into nuclei.

In any event, our studies on KN1 provide insights into some of the molecular events that orchestrate developmental processes in plants and identify one possible explanation for the plasticity of cell fate in the plant meristem (*2*).

REFERENCES AND NOTES

1. E. Huala and I. M. Sussex, *Plant Cell* **5**, 1157 (1993); I. M. Sussex, *Cell* **56**, 225 (1989).
2. W. J. Lucas, *Curr. Opin. Cell Biol.* **7**, 673 (1995).
3. R. Carpenter and E. S. Coen, *Development* **121**, 19 (1995); S. S. Hantke, R. Carpenter, E. S. Coen, *ibid.*, p. 27.
4. E. J. Symkowiak and I. M. Sussex, *Plant Cell* **4**, 1089 (1992).
5. W. J. Lucas, B. Ding, C. Van der Schoot, *New Phytol.* **125**, 435 (1993); W. J. Lucas and S. Wolf, *Trends Cell Biol.* **3**, 308 (1993).
6. W. J. Lucas and R. L. Gilbertson, *Annu. Rev. Phytopathol.* **32**, 387 (1994).
7. T. Fujiwara, D. Giesman-Cookmeyer, B. Ding, S. A. Lommel, W. J. Lucas, *Plant Cell* **5**, 1783 (1993); A. O. Noueiry, W. J. Lucas, R. L. Gilbertson, *Cell* **76**, 925 (1994); E. Waigmann, W. J. Lucas, V. Citovsky, P. Zambryski, *Proc. Natl. Acad. Sci. U.S.A.* **91**, 1433 (1994).
8. B. Ding, L. Qiubo, L. Nguyen, P. Palukaitis, W. J. Lucas, *Virology* **207**, 345 (1995).
9. S. Hake and M. Freeling, *Nature* **320**, 621 (1986); N. Sinha and S. Hake, *Dev. Biol.* **141**, 203 (1990); E. Vollbrecht, B. Veit, N. Sinha, S. Hake, *Nature* **350**, 241 (1991); L. G. Smith, B. Greene, B. Veit, S. Hake, *Development* **116**, 21 (1992).
10. In situ hybridization and immunolocalization experiments were performed on paraffin-embedded maize seedling apices. In situ hybridization was performed exactly as described (*11*), whereas for immunolocalization we used the method of Smith *et al.* (*9*), except that tissue was embedded in paraffin wax and sections were predigested with proteinase K (Sigma) at 100 μg/ml in phosphate-buffered saline (PBS) for 10 min at room temperature and then rinsed twice in PBS before the blocking step. Goat antibody to rabbit alkaline phosphatase (Boehringer Mannheim) was used as the secondary antibody (1:600 dilution) and visualized according to the method of Jackson *et al.* (*11*). Sections were lightly counterstained in basic fuchsin (0.005% w/v).
11. D. Jackson, B. Veit, S. Hake, *Development* **120**, 405 (1994).
12. Wild-type and mutant KN1 were expressed, extracted, and labeled with FITC according to the procedures we developed for viral movement proteins (*7*, *8*). As an internal control, proteins were extracted and FITC-labeled from an *E. coli* preparation that did not contain the *kn1* complementary DNA (cDNA). Alanine scanning mutants were created in groups of charged amino acids, which are likely to be present in surface domains (PC gene software, Intelligenetics). The *kn1* cDNA (Bam HI–Nco I partial digest) from pKOC10 was inserted into the pET23-d(+) vector (Novagen) to create pDJX-1. Single-stranded virions were produced in the CJ236 (*dut ung*) strain of *E. coli*, and site-directed mutagenesis was performed with oligonucleotides of 33 to 48 bases and with T7 DNA polymerase, according to the manufacturer's instructions (U.S. Biochemical). Mutagenized clones were confirmed by being sequenced before transfer to strain BL21(DE3) for protein production.
13. Microinjections were carried out essentially as previously described [S. Wolf, C. M. Deom, R. N. Beachy, W. J. Lucas, *Science* **246**, 377 (1989)], except for the modifications noted in (*7*, *8*).
14. N. Sinha, R. Williams, S. Hake, *Genes Dev.* **7**, 787 (1993).
15. A. W. Robards and W. J. Lucas, *Annu. Rev. Plant Physiol. Plant Molec. Biol.* **41**, 369 (1990).
16. E. Vollbrecht, R. Kerstetter, B. Lowe, B. Veit, S. Hake, in *Evolutionary Conservation of Developmental Mechanisms*, A. C. Spalding, Ed. (Wiley-Liss, New York, 1993), pp. 111–123; R. Kerstetter *et al.*, *Plant Cell* **6**, 1877 (1994); C. Lincoln, J. Long, J. Yamaguchi, K. Serikawa, S. Hake, *ibid.*, p. 1859.
17. *Kn1* sense or antisense RNA was transcribed with the use of T3 or T7 RNA polymerase from linearized pKOC10 plasmid that contained the full-length cDNA. The DNA template was digested with RQ1 DNase (Promega), and the RNA was phenol-extracted and ethanol-precipitated. *Kn1* RNA (1.6 kb) was resuspended in 20 μl of diethyl pyrocarbonate–H_2O, and concentration and purity were determined by spectroscopy. Sense and antisense RNA (500 μg/ml) were labeled with the nucleotide-specific fluorescent probe TOTO-1 (Molecular Probes) as previously described (*7*, *8*). All *kn1* RNA-TOTO preparations were adjusted to 225 μg/ml for use in microinjection experiments. CMV RNA-TOTO was adjusted to 250 to 500 μg/ml.
18. Purified CMV RNA was prepared [P. Palukaitis and M. Zaitlin, *Virology* **132**, 426 (1984)] and TOTO-labeled as described by Ding *et al.* (*8*). This preparation contained three single-stranded RNA species, RNA1 (3.3 kb), RNA2 (3.0 kb), and RNA3 (2.2 kb). The procedures of Ding *et al.* (*8*) were used to prepare and FITC-label the CMV 3a movement protein.
19. P. W. Becraft and M. Freeling, *Genetics* **136**, 295 (1994).
20. Single-letter abbreviations for the amino acid residues are as follows: A, Ala; C, Cys; D, Asp; E, Glu; F, Phe; G, Gly; H, His; I, Ile; K, Lys; L, Leu; M, Met; N, Asn; P, Pro; Q, Gln; R, Arg; S, Ser; T, Thr; V, Val; W, Trp; and Y, Tyr.

21. We thank P. Palukaitis of Cornell University for providing us with CMV RNA and the clone expressing the CMV 3a movement protein and M. Pfitzner for technical assistance with the color illustrations. Supported by NSF grant IBN-9406974 (W.J.L.) and U.S. Department of Agriculture CRIS 5335-21000-007-00D (S.H.).

7 August 1995; accepted 31 October 1995

Interaction of Tobamovirus Movement Proteins with the Plant Cytoskeleton

Manfred Heinlein, Bernard L. Epel,* Hal S. Padgett,† Roger N. Beachy‡

The movement protein of tobacco mosaic tobamovirus and related viruses is essential for the cell-to-cell spread of infection and, in part, determines the host range of the virus. Movement protein (MP) was fused with the jellyfish green fluorescent protein (GFP), and a modified virus that contained this MP:GFP fusion protein retained infectivity. In protoplasts and leaf tissues, the MP:GFP fusion protein was detected as long filaments shortly after infection. Double-labeling fluorescence microscopy suggests that the MP interacts and coaligns with microtubules. The distribution of the MP is disrupted by treatments that disrupt microtubules, but not by cytochalasin B, which disrupts filamentous F-actin. Microtubules may target the MP to plasmodesmata, the intercellular channels that connect adjacent cells.

Most, if not all, plant viruses direct the synthesis of one or more MPs required for the spread of infection from the initial site of infection to adjacent cells. It is generally thought that plant viruses circumvent the cell wall by exploiting plasmodesmata, specialized gatable channels that provide continuity between the cytoplasm of contiguous cells (*1*).

The most thoroughly studied virus-encoded MP is that of tobacco mosaic virus (TMV) (*2*, *3*). In plants infected with TMV or transgenically expressing MP, the MP is associated with plasmodesmata and increases their size exclusion limit (*4*, *5*). MP is targeted to the cell wall but is also found associated with the plasma membrane and

The Scripps Research Institute, Department of Cell Biology, MRC7, 10666 North Torrey Pines Road, La Jolla, CA 92037, USA.

*Permanent address: Botany Department, Tel Aviv University, Tel Aviv 69978, Israel.
†Permanent address: Division of Biology and Biomedical Sciences, Washington University, St. Louis, MO 63110, USA.
‡To whom correspondence should be addressed. E-mail: beachy@scripps.edu